

Received: 2018.01.24
Accepted: 2018.03.07
Published: 2018.09.02

Use of Apparent Diffusion Coefficient Histogram in Differentiating Between Medulloblastoma and Pilocytic Astrocytoma in Children

Authors' Contribution:
Study Design A
Data Collection B
Statistical Analysis C
Data Interpretation D
Manuscript Preparation E
Literature Search F
Funds Collection G

ABCDEF **Weijian Wang**
ACDE **Jingliang Cheng**
BCDEF **Yong Zhang**
BCDEF **Chaoyan Wang**

Magnetic Resonance Imaging (MRI) Division, The First Affiliated Hospital of Zhengzhou University, Zhengzhou, Henan, P.R. China

Corresponding Author: Jingliang Cheng, e-mail: jingliangcheng1@sina.com
Source of support: Departmental sources

Background: This research aimed to investigate the value of apparent diffusion coefficient (ADC) histogram in differentiating between medulloblastoma and pilocytic astrocytoma in children.





Material/Methods: Thirty-three children with posterior cranial fossa tumor confirmed by operation and pathology participated in this retrospective study, including 18 children with medulloblastoma and 15 children with pilocytic astrocytoma. ADC images of the maximum layer of tumors were selected, and the region of interest was delineated by Mazda software and analyzed by histogram. Histogram characteristic parameters of the 2 tumors were statistically analyzed to determine the significantly different characteristic parameters between the 2 tumor types.

Results: There were significant differences in the mean value, variance, skewness, kurtosis, and 1th, 10th, 50th, and 90th percentiles of 9 characteristic parameters extracted by histogram ($P < 0.05$). The corresponding receiver operating characteristic (ROC) curves were drawn, in which the mean value and 50th percentile were best identified. When the maximum area under the ROC curve was 1 and the optimal threshold was 137.7 and 125.5, the specificity and sensitivity were both 100%.

Conclusions: ADC histograms can be used to differentiate between medulloblastoma and pilocytic astrocytoma in children and provide reliable and objective evidence for the differentiation.

MeSH Keywords: **Astrocytoma • Magnetic Resonance Imaging • Medulloblastoma**

Full-text PDF: <https://www.medscimonit.com/abstract/index/idArt/909136>

 1916  2  1  24



Background

Central nervous system (CNS) tumors are the second most common tumor in children; 50% of pediatric intracranial tumor occur in the posterior cranial fossa. Pilocytic astrocytoma and medulloblastoma are the 2 most common tumors [1]. Pilocytic astrocytoma is a WHO I-level tumor [2] with low mitotic activity and very low malignant transformation potential. Medulloblastoma, a WHO IV-level tumor, is a common invasive embryonic tumor in the cerebellum of children. The 2 tumors often have an onset before the age of 15. It is difficult to some extent to evaluate posterior cranial fossa tumors by conventional brain magnetic resonance imaging (MRI), and apparent diffusion coefficient (ADC) is considered to be an important auxiliary method [3–5] because it is significantly more sensitive to partial solid tumor cells characteristics [6]. Thus, ADC histograms are used to differentiate different types of tumors. The method includes the measurement of average ADC value [7] and the minimum ADC value [8] of the tumor. ADC value is usually measured in the solid portion of the tumor [9]. Because both pilocytic astrocytoma and medulloblastoma have obvious cystic parts, ADC values cannot fully reflect the tumor condition, and it is unreliable to identify tumor types or grades by ADC value alone. The histogram can be used to analyze the whole tumor volume and is less dependent on the tumor microstructure and small sample of the region of interest (ROI) [10]. ADC histogram shows the frequency of ADC values and provides more descriptive information outside the average ADC value. ADC histograms have been applied to distinguish adult brain tumors, especially low-grade gliomas, pilocytic astrocytoma, and oligodendroglioma [11]. Thirty-three children with posterior cranial fossa medulloblastoma and pilocytic astrocytoma confirmed by operation and pathology were enrolled in this retrospective study. ADC histogram characteristics of the 2 tumors were analyzed based on the magnetic resonance ADC image data. The identification value of ADC histograms to the 2 tumors was evaluated by extracting the image information, which was not visible to the naked eye.

Material and Methods

Basic data

This retrospective study was approved by the Institutional Ethics Review Committee of our hospital. The data of 33 children with posterior cranial fossa tumors confirmed by operation and pathology from June 2011 to June 2016 in our hospital were analyzed. The main clinical manifestations were headache, dizziness, emesis, and standing instability. The inclusion criteria were: (1) medulloblastoma and pilocytic astrocytoma confirmed by operation and pathology; (2) preoperative

conventional MRI examination in our hospital, including axial surface T₁WI, T₂WI, FLAIR (fluid attenuated inversion recovery), DWI (diffusion weighted imaging), ADC, and enhanced T₁WI; and (3) no obvious artifacts affecting further image analysis on MRI images.

Magnetic resonance imaging methods

We used the Siemens Trio TIM 3.0T magnetic resonance imaging system (Germany) and standard head coil. The patient was relaxed naturally in supine position and maintained the forehead and face in horizontal position and the nose root in the central line of the coil. Plain scan in sagittal and axial position T₁WI, T₂WI, FLAIR sequence, and b value of axial DWI (0, 800 s/mm²) were performed. Enhanced scan in sagittal, axial, and coronal positions T₁WI were performed with 0.1 mmol/kg of Gd-DTPA as a contrast medium. Scanning parameters were: T₁WI: TR 260.0 ms, TE 2.46 ms; T₂WI: TR 3800 ms, TE 93.0 ms; FLAIR: TR 4500 ms, and TE 93.0 ms. DWI scanning was carried out by SE-EPI sequence, with b=0 and 1000 s/mm², TR 3500 ms, TE 119 ms; 23×23cm field of vision, 5-mm-layer thick, 0.3-mm-layer spacing, and 20 layers.

ROI selection

Image selection

MRI images of all patients were exported from PACS workstation in BMP format. The window width and window position were adjusted when exported, so that all images had consistent window width and window position and were saved on the hard disk. ROI on ADC image was selected for further analysis by reference to T₁WI, T₂WI, and T₁WI enhanced images.

Histogram analysis

MaZda software was used to analyze the image of the largest lay of selected lesions. ROI was delineated manually to calculate histogram parameters including mean value, variance, skewness, kurtosis, and percentile values. It was easier for the experimenter to learn how to use the software, and the software package ran stably in Windows 7. The process of texture features calculation and evaluation was as follows: 1 physician delineated ROI manually along the edge of the lesion, and the tumor region was delineated on one of the samples and filled with red. The corresponding images before and after marking are shown in Figure 1.

Statistical analysis

SPSS 21.0 statistical software was applied to analyze the data. If the data conformed to normal distribution, the 2 independent-samples *t* test was used to compare the difference in

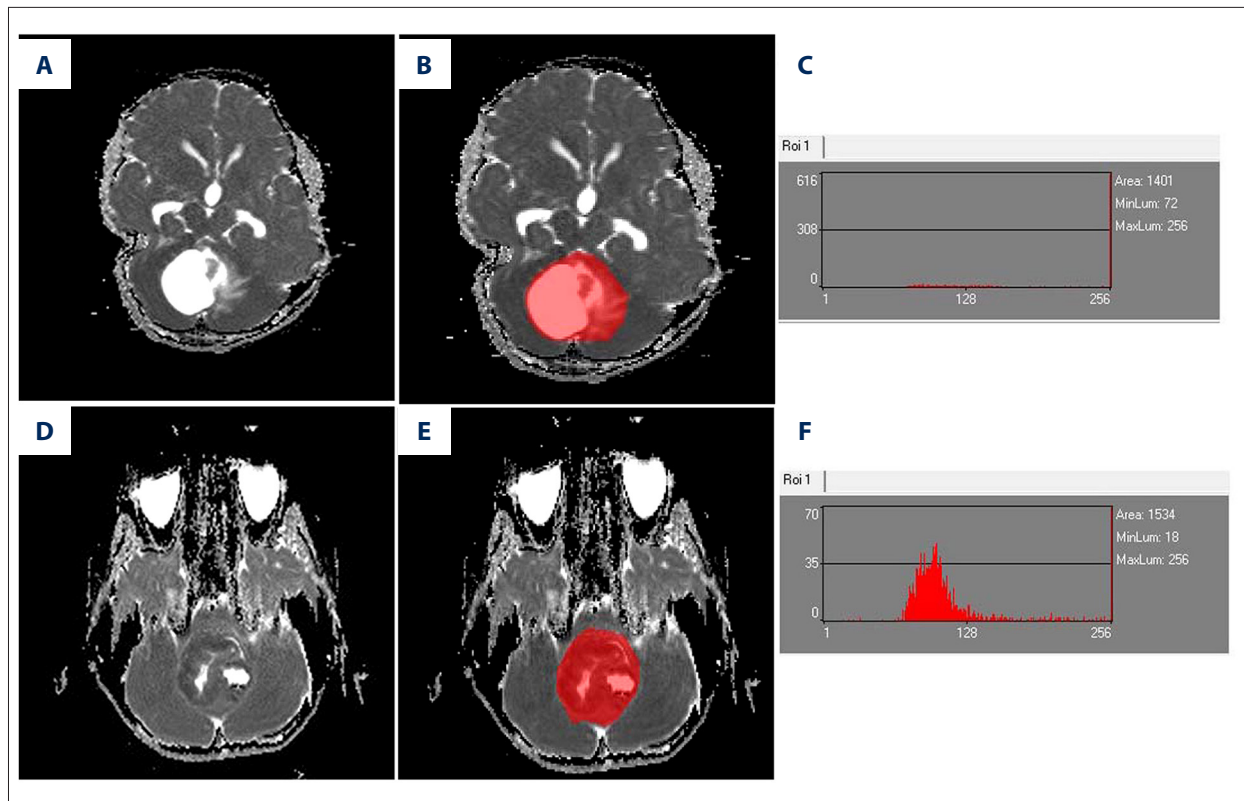


Figure 1. ROI and histogram of pilocytic astrocytoma (A–C) and medulloblastoma (D–F). ROI – region of interest.

each parameter between the 2 kinds of histograms. If the data did not conform to normal distribution, the non-parametric test was used. There was a significant difference at $P < 0.05$. Receiver operating characteristic (ROC) curves were drawn, and the area under the curve was calculated. The optimal threshold value of medulloblastoma and pilocytic astrocytoma in central line of the cerebellum was predicted, which was determined by the maximum value.

Results

Basic data

In this research, there were 18 patients with medulloblastoma, including 15 males and 3 females, ages 3–15 years with an average age of 8.8 ± 3.3 , and 15 patients with pilocytic astrocytoma, including 8 males and 7 females, ages 3–13 years with an average age of 6.8 ± 3.0 . There were no differences in age, sex, or tumor size between the 2 tumor types (Table 1).

ADC histogram results

The results of ADC histograms are shown in Table 2. The skewness and kurtosis of medulloblastoma were higher than those of pilocytic astrocytoma ($P = 0.000$, $P = 0.001$), with a significant

difference. The mean value, variance, and 1th, 10th, 50th, and 90th percentiles of medulloblastoma were lower than those of pilocytic astrocytoma, with a significant difference, and there was no significant difference in the 99th percentile ($P = 0.055$). The mean value and the 50th percentile were best identified. When the maximum area under the ROC curve was 1, and the optimal threshold was 137.7 and 125.5, the specificity and sensitivity were both 100%.

Discussion

The cystic part of a cerebellar pilocytic astrocytoma contains many protein components, so the T_1 WI signal is often equal to or higher than the cerebrospinal fluid signal. “There is a tumor in the sac and a sac in the tumor” is its characteristic image manifestation. Medulloblastomas had a homogeneous low T_1 WI signal and equal high T_2 WI signal. Multiple small cystic lesions were seen on the edge of tumors, and enhancement scan was enhanced unevenly. Pierce et al. [12] confirmed that ADC value of pilocytic astrocytoma was higher than that of medulloblastoma, and that the 2 tumors could be differentiated and diagnosed by ADC difference and DWI. Moreno-Torres et al., in a study of 14 patients [13], found that the peak of taurine of medulloblastomas was higher than that of pilocytic astrocytomas as shown by magnetic resonance spectroscopy (MRS),

Table 1. Characteristics of patients with medulloblastoma and pilocytic astrocytoma in children.

Term	Pilocytic astrocytoma	Medulloblastoma	P
Number of patients	15	18	
Age, yr	6.8±3.0	8.8±3.3	0.073
Gender	Male	15	0.074
	Female	3	
Number of tumor	15	18	
Solitary	15	18	
Tumor size, mm	41.8±14.6	37.0±9.3	0.268
Location	Fourth ventricle	13	0.143
	cerebellum	5	

Table 2. Histogram data of pilocytic astrocytoma and medulloblastoma.

	Pilocytic astrocytoma	Medulloblastoma	P	AUC (95% CI)
Mean	200.9±31.4	106.5±15.8	<0.001	1.000 (1.000–1.000)
Variance	2632.5±1029.2	1670.6±1112.6	0.027	0.726 (0.549–0.903)
Skewness	-0.9±1.1	2.2±0.8	<0.001	0.974 (0.921–1.00)
Kurtosis	1.0±2.1	6.5±5.6	0.001	0.822 (0.682–0.963)
1%	76.7±21.9	62.6±8.7	0.031	0.754 (0.569–0.939)
10%	120.1±28.2	75.5±8.5	<0.001	0.983 (0.949–1.000)
50%	219.0±41.2	94.1±11.6	<0.001	1.000 (1.000–1.000)
90%	243.2±25.6	160±53.9	<0.001	0.893 (0.780–1.000)
99%	254.9±4.1	237.9±31.2	0.055	0.641 (0.452–0.830)

AUC – the area under the receiver operating characteristic curve; CI – confidence intervals.

and that DWI combined with MRS could also differentiate the 2 tumors [14]. However, not all hospitals have the equipment needed to carry out these sequences, and the cost is high.

DWI provides image contrast based on differences in water molecular diffusion characteristics in the brain [15]. Diffusion displays the random motions of water molecules, and the influencing factors include molecular type, tissue temperature, and diffusion-occurring micro-environment [16]. ADC value shows the absolute value of the measured diffusion amount. On ADC histograms, low ADC values indicate limited diffusion, while high ADC values indicate increased diffusion. DWI and ADC are widely used in brain tumor detection, including: (1) grading and histological subtype determination, (2) evaluation of tumor edema and tumor infiltration pathway, (3) quantitative measurement and monitoring of treatment responses, and (4) identification of necrotic tissue and tumor recurrence (e.g., radiotherapy and chemotherapy) [17–20]. Because ADC excludes cystic components in sampling ROI, it cannot reflect the entire tumor information. In addition, ADC values are widely

overlapped, so it is unreliable to identify tumor types or grades by ADC value alone. Therefore, we used ADC histograms to analyze the characteristics of the whole tumor.

In this research, the histogram was used to analyze and evaluate the mean value, variance, skewness, kurtosis, and 1th, 10th, 50th, 90th, and 99th percentiles to reflect the distribution of ADC values. The histogram skewness described the distribution symmetry of variable values, indicating the distribution asymmetry degree relative to the mean value [21]. The positive skewness indicated that the asymmetric tail of the distribution tended to larger values, and the distribution's body was centered on the right side, while the vast majority of values (including the median) were on the left side of the mean value. The negative skewness indicated that the asymmetric tail of the distribution tended to smaller values. The larger the absolute value of skewness, the greater the skewing of distribution form. The kurtosis of histograms was the statistic describing the distribution steep degree of all values in the whole, which reflected the relative sharpness or flatness

of a distribution compared with normal distribution. A positive peak indicated a sharper distribution than normal distribution and a negative peak indicated a flatter distribution than normal distribution. In this research, the skewness and kurtosis of medulloblastoma were higher than those of pilocytic astrocytoma. The skewness and kurtosis of ADC histograms significantly distinguished between pilocytic astrocytoma and medulloblastoma, which was consistent with the research results of Wagner et al. [10]. Medulloblastomas were more heterogeneous.

The histogram technique reflected different tissue compositions in the tumor body by measuring all voxels of the tumor. The corresponding data of percentiles were less than or equal to this percentile, indicating that there were differences in all voxels of the tumor between medulloblastomas and pilocytic astrocytomas, which reflected the different tissue compositions of these 2 tumor types. It was reported that the voxels of low ADC value had a good correlation with high cell compositions in the tumor. The higher the ADC value, the higher the voxel frequency, which reflected mucoprotein or necrosis [22–24]. Medulloblastomas were composed of highly dense small cells, with less extracellular matrix, increased diffusion restriction, and lower ADC value. Pilocytic astrocytoma was composed of dense bipolar tumor cells, containing Rosenthal fibers and acidophilic body, with larger intercellular space, less diffusion restriction, and higher ADC value. Therefore,

pilocytic astrocytoma had high voxel frequency. The mean value and percentiles of pilocytic astrocytoma were higher than those of medulloblastoma. ADC histogram parameters could reflect the pathological characteristics of medulloblastoma and pilocytic astrocytoma. In this research, all ADC histogram parameters had significance for differentiation, except for the 99th percentile.

There are some limitations in our research. First, it is a small-scale retrospective study in which the number of patients with each tumor type was unbalanced. In this research, we focused on the 2 most common tumors in the posterior cranial fossa of children. We did not investigate other tumors, such as ependymomas, hemangioblastomas, and atypical teratoid/rhabdoid tumors. Second, the sample size was small, and further research is needed to enlarge the sample size. There is no further classification of medulloblastoma, which needs further study. The correlation between ADC histogram parameters and histopathological characteristics needs further study.

Conclusions

To sum up, our research shows that use of ADC histograms is a non-invasive method that synthesizes all voxels of the entire tumor volume to obtain histogram data. The results are more objective and accurate and can better differentiate between medulloblastomas and pilocytic astrocytomas in the posterior cranial fossa of children.

References:

1. Zitouni S, Koc G, Doganay S et al: Apparent diffusion coefficient in differentiation of pediatric posterior fossa tumors. *Jpn J Radiol*, 2017; 35: 448–53
2. Louis DN, Ohgaki H, Wiestler OD et al: The 2007 WHO classification of tumours of the central nervous system. *Acta Neuropathol*, 2007; 114: 97–109
3. Chen Z, Ma L, Lou X, Zhou Z: Diagnostic value of minimum apparent diffusion coefficient values in prediction of neuroepithelial tumor grading. *J Magn Reson Imaging*, 2010; 31: 1331–38
4. Rumboldt Z, Camacho DL, Lake D et al: Apparent diffusion coefficients for differentiation of cerebellar tumors in children. *Am J Neuroradiol*, 2006; 27: 1362–69
5. Razeq A, El-Serougy L, Abdelsalam M et al: Differentiation of residual/recurrent gliomas from postradiation necrosis with arterial spin labeling and diffusion tensor magnetic resonance imaging-derived metrics. *Neuroradiology*, 2018; 60: 169–77
6. El-Serougy L, Abdel Razeq AA, Ezzat A et al: Assessment of diffusion tensor imaging metrics in differentiating low-grade from high-grade gliomas. *Neuroradiol J*, 2016; 29: 400–7
7. Gimi B, Cederberg K, Derinkuyu B et al: Utility of apparent diffusion coefficient ratios in distinguishing common pediatric cerebellar tumors. *Acad Radiol*, 2012; 19: 794–800
8. Ji YM, Geng DY, Huang BC et al: Value of diffusion-weighted imaging in grading tumours localized in the fourth ventricle region by visual and quantitative assessments. *J Int Med Res*, 2011; 39: 912–19
9. Poretti A, Meoded A, Cohen KJ et al: Apparent diffusion coefficient of pediatric cerebellar tumors: a biomarker of tumor grade? *Pediatr Blood Cancer*, 2013; 60: 2036–41
10. Wagner MW, Narayan AK, Bosemani T et al: Histogram analysis of diffusion tensor imaging parameters in pediatric cerebellar tumors. *J Neuroimaging*, 2016; 26: 360–65
11. Tozer DJ, Jäger HR, Danchaiwitt N et al: Apparent diffusion coefficient histograms may predict low-grade glioma subtype. *NMR Biomed*, 2007; 20: 49–57
12. Pierce TT, Provenzale JM: Evaluation of apparent diffusion coefficient thresholds for diagnosis of medulloblastoma using diffusion-weighted imaging. *Neuroradiol J*, 2014; 27: 63–74
13. Moreno-Torres A, Martínez-Pérez I, Baquero M et al: Taurine detection by proton magnetic resonance spectroscopy in medulloblastoma: Contribution to noninvasive differential diagnosis with cerebellar astrocytoma. *Neurosurgery*, 2004; 55: 824–29; discussion 829
14. Schneider JF, Confort-Gouy S, Viola A et al: Multiparametric differentiation of posterior fossa tumors in children using diffusion-weighted imaging and short echo-time 1H-MR spectroscopy. *J Magn Reson Imaging*, 2007; 26: 1390–98
15. Huisman TA: Diffusion-weighted and diffusion tensor imaging of the brain, made easy. *Cancer Imaging*, 2010; 10 Spec no A: S163–71
16. Huisman TA: Diffusion-weighted imaging: Basic concepts and application in cerebral stroke and head trauma. *Eur Radiol*, 2003; 13: 2283–97
17. Rahman R, Hamdan A, Zweifler R et al: Histogram analysis of apparent diffusion coefficient within enhancing and nonenhancing tumor volumes in recurrent glioblastoma patients treated with bevacizumab. *J Neurooncol*, 2014; 119: 149–58
18. Pope WB, Kim HJ, Huo J et al: Recurrent glioblastoma multiforme: ADC histogram analysis predicts response to bevacizumab treatment. *Radiology*, 2009; 252: 182–89

19. Chenevert TL, Ross BD: Diffusion imaging for therapy response assessment of brain tumor. *Neuroimaging Clin N Am*, 2009; 19: 559–71
20. Provenzale JM, Mukundan S, Barboriak DP: Diffusion-weighted and perfusion MR imaging for brain tumor characterization and assessment of treatment response. *Radiology*, 2006; 239: 632–49
21. Shindo T, Fukukura Y, Umanodan T et al: Histogram analysis of apparent diffusion coefficient in differentiating pancreatic adenocarcinoma and neuroendocrine tumor. *Medicine (Baltimore)*, 2016; 95: e2574
22. Woo S, Cho JY, Kim SY, Kim SH: Histogram analysis of apparent diffusion coefficient map of diffusion-weighted MRI in endometrial cancer: A preliminary correlation study with histological grade. *Acta Radiol*, 2014; 55: 1270–77
23. Kang Y, Choi SH, Kim YJ et al: Gliomas: Histogram analysis of apparent diffusion coefficient maps with standard- or high-b-value diffusion-weighted MR imaging – correlation with tumor grade. *Radiology*, 2011; 261: 882–90
24. Downey K, Riches SF, Morgan VA et al: Relationship between imaging biomarkers of stage I cervical cancer and poor-prognosis histologic features: Quantitative histogram analysis of diffusion-weighted MR images. *Am J Roentgenol*, 2013; 200: 314–20